Experimental Analysis of Steady-State Maneuvering Effects on Transmission Vibration Patterns Recorded in an AH-1 Cobra Helicopter

Edward M. Huff and Eric Barszcz
NASA Ames Research Center
Moffett Field, CA
ehuff@mail.arc.nasa.gov

Irem Y. Tumer
Caelum Research Corporation
NASA Ames Research Center
Moffett Field, CA

Mark Dzwonczyk and James McNames[1]
California Signal Processing Associates, Inc.
Los Altos, CA

ABSTRACT

During the past several years, an AH-1 Cobra aircraft at the NASA Ames Research Center has been instrumented with tri-axial accelerometers and a data acquisition system to support the experimental study of in-flight transmission vibration patterns. This paper describes the on-board *HealthWatch* system and presents some important initial statistical analyses of the collected data sets. These analyses provide insight into how transmission vibration responds to several factors typically related to health and usage monitoring (HUMS), such as maneuver condition, order of execution, and pilot differences. Although a large database of flight recordings has been collected, these results focus on an overall analysis of planetary ring gear data that were recorded in two sets of flights. It is shown that RMS variability due to torque is a major factor to be considered in real-time HUMS design and that certain steady state maneuvers yield a dramatically higher percentage of stationary recordings. Finally, it is conjectured that multi-axis recording may have previously unrecognized advantages for signal conditioning or analysis.

INTRODUCTION

A significant body of research exists concerning the vibration patterns of rotorcraft drive trains using test stand data [1-4], yet there is a dearth of results from data gathered in flight. A welcome exception is the work recently reported by Hess *et al* [5] involving the use of an SH-60 iron-bird ground simulator for comparison with test aircraft. While it would be desirable to apply engineering knowledge or test stand results directly to the flight situation, vehicle state, environmental conditions, and maneuvering forces can be expected to have important, yet poorly understood, effects on observed vibration patterns. Furthermore, many sources of aircraft vibration that are present in flight, such as the engine, main rotor, and tail rotor, make vibration recordings more difficult to analyze or interpret than those simply collected from isolated test rigs.

A basic series of flight studies is currently being conducted at the NASA Ames Research Center (ARC) to collect reference data and to explore the extent of these effects. This paper reports on the analysis of vibration data collected from a two-phase flight experiment that was completed in May 1999 on the Flying Laboratory for Integrated Test and Evaluation (FLITE), which is a Cobra AH-1 rotorcraft maintained by the US Army at Ames (Fig.1). Specifically, this paper describes overall experiment-wide findings regarding the statistical stationarity of transmission vibrations during the various maneuvering conditions, as well as the outcome of several linear regression and analysis-of-covariance (ANCOVA) models. These analyses are limited to data collected from the planetary ring gear. Results concerning data collected at the input pinion will be reported at a future time. For research purposes, vibration recordings were made using tri-axial accelerometers, hence, preliminary multi-axis vibration response characteristics are also reported.

[1] Currently at Portland State University.

Presented at the American Helicopter Society 56th Annual Forum, Virginia Beach, Virginia, May 2-4, 2000.

Figure 1. ARC's Flying Laboratory for Integrated Test and Evaluation (FLITE)

OBJECTIVES

The present flight experiment was designed primarily to determine the extent to which steady-state maneuvers influence characteristic vibration patterns measured at the input pinion and output planetary gear locations of a main helicopter transmission. The overall objective was to develop a better understanding about the manner in which several inter-related factors contribute to the size and variability of the vibration signals, and possibly to identify the most satisfactory flight conditions under which to acquire data for continuous on-board HUMS applications.

As a whole, the research sought to determine if certain maneuvers systematically influence vibration patterns—knowledge that might be used to detect and recognize aberrant signals associated with the growth of internal transmission damage. The study was also designed to collect a library of baseline flight data and to develop methods for comparison of flight data with data obtained from test stands at Glenn Research Center (GRC).[2] Finally, because this was the first vibration study on the Cobra aircraft, considerable effort was invested in developing an in-flight recording apparatus, exploring acceleration mounting methods, and generally learning about the overall vibratory characteristics of the aircraft itself.

[2] Since this study was completed, provision was made to instrument an Ames OH-58c helicopter for comparison of flight data with data from GRC's OH-58c transmission test stand.

METHOD

Aircraft Instrumentation

The Cobra was instrumented as shown in Fig. 2. A data acquisition system (*HealthWatch*), located in the tail boom, was designed specifically for this application and recorded eight-channels of analog data. Two three-axis Endevco model 7253A-10 accelerometers, denoted A and B, were positioned initially at the planetary ring gear (annulus) and input pinion gear locations respectively. The accelerometers were screw-mounted on specially fabricated brackets which were threaded onto existing transmission housing bolts. In addition to the six accelerometer channels, one channel was used for sampling a once-per-revolution tachometer pulse from the main rotor shaft. The remaining channel was used for engine torque.

Accounting for the resonant frequency of the accelerometer mounting bracket, which was analytically estimated to be 23kHz, appropriate order anti-aliasing filters were used in combination with a per-channel sampling rate of 50kHz to satisfy the Nyquist sampling conditions. In addition to analog data, time correlated aircraft attitude data were also obtained from a MIL-STD-1553 serial data bus. These included, radar altitude, airspeed, rate-of-climb, heading, bank angle, pitch angle, and side slip.

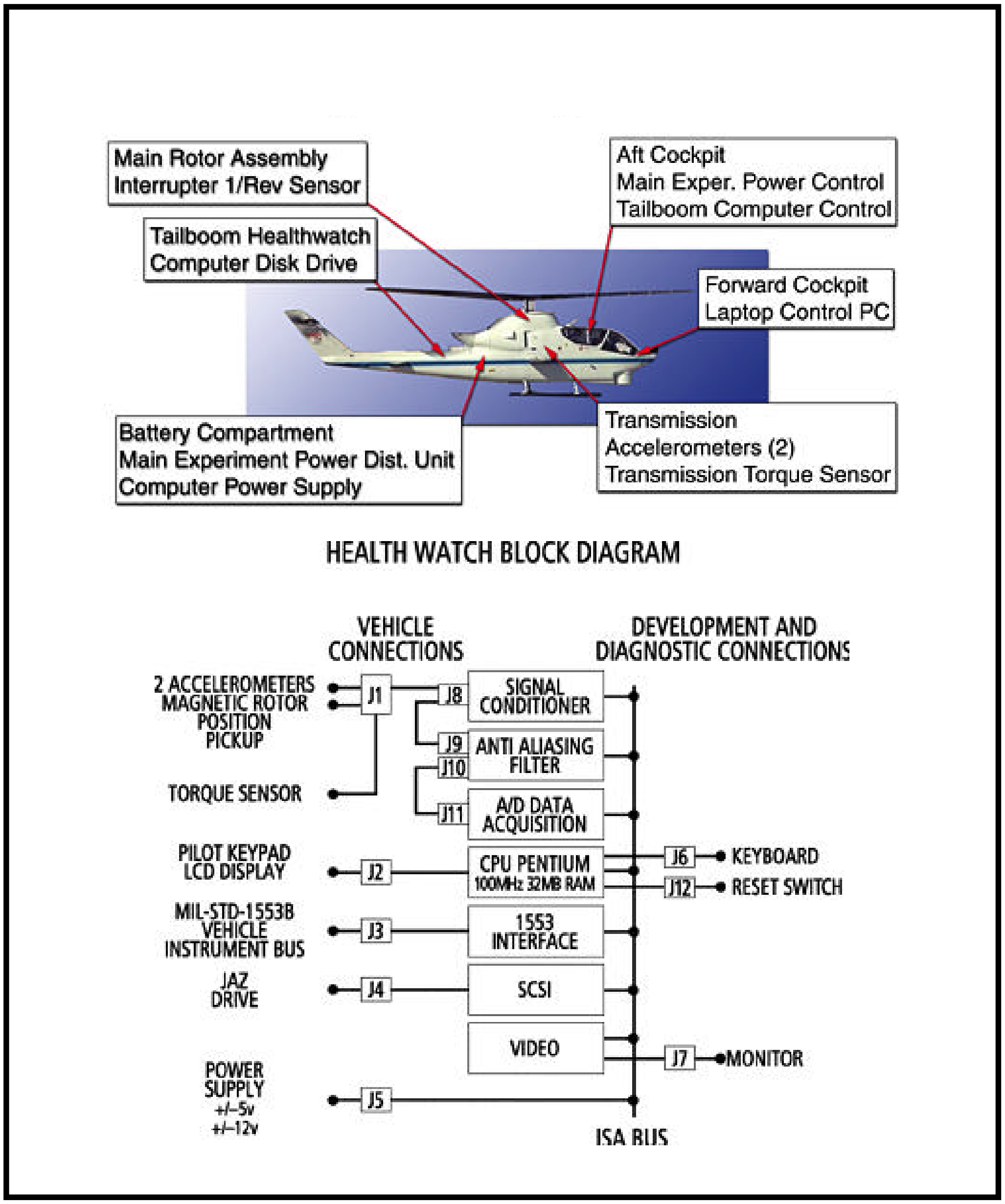

Figure 2. Aircraft Instrumentation

Accelerometer Validation and Gain Settings

During an early test flight prior to the experiment, what were thought to be excessively high peak-to-peak g-levels were observed at both the pinion (±500g) and planetary (±250g) locations. Such high levels exceeded the dynamic range of the accelerometers and signal clipping occurred. Since the open literature was not informative in this regard, there was some concern initially that the observations were due to a recording artifact.[3] As a direct result of this conjecture, accelerometer B (channels 4-6) was moved to a new location at some distance from the mesh contact point of the input pinion gear where it was originally placed.

As shown in Table 1, there was a beneficial effect of moving accelerometer B: the RMS of the signal was lower at the new location thus allowing the accelerometers to be used with only occasional clipping. For the experiment, the gains on the signal conditioning board were set at ±250g, except for channels 4 and 5, which were set to ±500 while it was mounted near the pinion gear during Phase 1.

[3] Published vibration levels were not found for any helicopter transmission.

Table 1: RMS (g-level) for Three Maneuver-F recordings

Channel	Test Flight	Flight 1	Flight 3	Flight 3
1	27.86	34.57	33.84	32.77
2	20.03	20.98	22.10	22.80
3	12.55	15.39	14.57	14.61
4	64.74	86.52	74.87	76.94
5	198.73	128.01	123.69	127.63
6	23.37	21.59	19.97	19.70

The conclusion that high g-levels are an *inherent* aspect of a Cobra transmission, and not an anomaly due to our accelerometers or data recording system, was further corroborated by an independent shake-table test. The highly consistent output of each accelerometer channel is shown for a known peak amplitude of 30g (Table 2). In general, all channels were found to be highly linear and independent up to the shake-table limit of 30g. Hence, there was no reason to believe that the accelerometer or the data acquisition system would account for the observed signal amplitudes.

Table 2: Shake Table Results (g-level)

Channel	RMS	RMS $\times\sqrt{2}$	Peak
1	21.72	30.72	31.13
2	21.91	30.99	31.74
3	22.08	31.23	31.37
4	22.38	31.65	33.20
5	21.75	30.76	31.25
6	21.96	31.06	31.74

Experiment Design

The experiment was conducted in two phases, each composed of a set of four flights flown on successive days. Phase 1 was completed in Oct. 1998 and Phase 2 in May 1999. In each set of flights, the same pilots flew the aircraft in various steady-state maneuvers (Table 3), according to a pre-determined test matrix (Table 4). This test matrix utilized a modified Latin-square design to counterbalance random wind conditions, ambient temperature, and fuel depletion.

At the start of each flight a recording was first taken on the ground (Maneuver G) with the blades at flat pitch, and a second recording was taken in flight at low hover (Maneuver H). These and the 12 primary flight maneuvers were each scheduled to last 34 seconds in order to allow sufficient number of cycles of the main rotor and planetary gear assembly to apply known signal decomposition techniques to the recorded signals. In each phase of the experiment, therefore, 72 raw data records of 34 seconds were obtained for the primary flight maneuvers: 12 maneuvers, flown by two pilots, on three separate occasions. Counting the 16 aggregate hover and ground recordings taken at the start and end of each flight, a grand total of 88 recordings were obtained per flight set, or 176 recordings for the complete two-phase experiment. It may be noted that since each of eight analog channels was sampled at 50kHz, and correlated 1553 Bus data were also taken from the bus, a massive amount of data was collected on each flight. This was stored on a high-density removable (Jaz) cartridge and archived at the end of the flight.

During Phase-1, the two three-axis accelerometers were mounted near the planetary ring and input pinion gears respectively. During Phase-2, the accelerometer near the input pinion was moved to a second location at the planetary ring gear with appropriate changes made in gain. Although analyses of the second accelerometer are not reported here, this made it possible to obtain reference data to explore the merits of a two-element "sensor array" to decompose the highly complex planetary signals. In all other respects, Phase-1 and -2 were conducted in exactly the same manner.

Table 3: Aircraft Maneuvers for Phases 1 and 2

Maneuver	Name	Symbol	Description
A	Forward Flight, Low Speed	FFLS	Fly straight, level, & forward at ~ 20 kts.
B	Forward Flight, High Speed	FFHS	Fly straight, level, & forward at ~ 60 kts.
C	Sideward Flight Left	SL	Fly straight, level, & sideward left.
D	Sideward Flight Right	SR	Fly straight, level, & sideward right.
E	Forward Climb, Low Power	FCLP	Fly forward, straight, & climb at 40 psi.
F	Forward Descent, Low Power	FDLP	Fly forward, straight, & descend at 10 psi.
G	Flat Pitch on Ground	G	Vehicle on ground skids.
H	Hover	H	Stationary hover.
I	Hover Turn Left	HTL	Level hover, turning left.
J	Hover Turn Right	HTR	Level hover, turning right.
K	Coordinated Turn Left	CTL	Fly level, forward, & turning left.
L	Coordinated Turn Right	CTR	Fly level, forward, & turning right.
M	Forward Climb, High Power	FCHP	Fly forward, straight, & climb at 50 psi.
N	Forward Descent, High Power	FDHP	Fly forward, straight, & descend at 50 psi.

Table 4: Flight Protocol for Each Phase of Experiment

		Obs. Order	Ground & Hover		Primary Flight Maneuvers						Hover & Ground	
Pilot 1	Flight 1	1	G	H	A	B	C	D	E	F		
		2			B	C	D	E	F	A		
		3			C	D	E	F	A	B	H	G
	Flight 2	1	G	H	I	J	K	L	M	N		
		2			J	K	L	M	N	I		
		3			K	L	M	N	I	J	H	G
Pilot 2	Flight 3	1	G	H	D	E	F	A	B	C		
		2			E	F	A	B	C	D		
		3			F	A	B	C	D	E	H	G
	Flight 4	1	G	H	L	M	N	I	J	K		
		2			M	N	I	J	K	L		
		3			N	I	J	K	L	M	H	G

RESULTS

Conceptual Causal Model

The analyses presented below were conceptualized within the general framework of an open-loop causal model (Fig. 3). In this model it may be noted that the various maneuvers, {M}, are thought to induce the set of observable aircraft attitudes, {A}, which induce *potentially* observable inputs, {I}, to the transmission. The internal responses, {R}, that occur within the transmission itself are not directly observable, but produce measurable outputs {O}. Since we assume, by hypothesis, that the specimen aircraft under study had no transmission damage, the results presented here were thought to be only determined by these causal relationships—plus additional random or uncontrolled factors such as turbulence or other environmental conditions. If the transmission were damaged to some small extent, however, these effects would have been combined in some complex manner within the output set {O}. In a general sense, then, the knowledge gained from this kind of empirical research is hoped to separate what is predictable from what is not, and lay the groundwork for early detection of internal damage.

Flight Maneuver {M}	Aircraft Attitude {A}	Physical Input {I}	Internal Response {R}	Measured Output {O}
· Fwd. Flight · Side Flight · Fwd. Climb · Fwd. Descent · Hover · Hover Turn · Coord. Turn · *[other]*	· Radar Alt. · Airspeed · Climb Rate · Heading · Bank · Pitch · Side Slip · *[other]*	· Engine Torque · Engine Speed · *[Mast Lifting]* · *[Mast Bending]* · *[other]*	· *[Tooth Bending]* · *[Backlash]* · *[Friction]* · *[Heat]* · *[other]* · *[DAMAGE]*	· Vibration - x axis - y axis - z axis · *[Temp.]* · *[Noise]* · *[other]*

Figure 3. Conceptual open-loop model illustrating assumed causal relationships

The Use of RMS for Assessing Vibration Responses

The analyses reported here use only the RMS of the vibration time series for global univariate analysis, even though eventual interest lies in isolating and identifying spectral *patterns*. The reasoning behind this is based on the general relationship:

$$RMS = \sqrt{\sum_i P_i}$$

where P_i is the power of the ith frequency bin of the DFT. Clearly, although it is theoretically possible for the relative spectral distribution to remain constant while total power, $\sum_i P_i$, changes, this circumstance is not likely to occur in practice. In virtually all cases, observed differences in RMS will correspond to differences in the spectral distribution, and these, in turn, should be identifiable in the frequency or time-frequency domains.

Data Reduction

To facilitate the statistical analyses, the data were reduced in two stages. Each stage produced highly compressed summary information, which has been archived as a derived database and is available for continued analyses. In the first stage, the basic statistical properties of each 34 sec. recording of raw flight data were consolidated into summary matrices (SMs). This was done entirely in the time domain by calculating the first four moments of each parameter, including the 1553 Bus information, on a revolution-by-revolution basis. Because each recording had at least 178 revolutions, each SM, is a 178 x p matrix, where the p columns containing the mean, standard deviation (or RMS), skew and kurtosis of the various parameters for one shaft revolution. Since each shaft revolution took approximately 0.2 sec., and sampling occurred at 50 kHz, approximately 10,000 data points were compressed into each summary statistic in the summary matrix. The number of data counts for each revolution was used to calculate an RPM measure of the rotor shaft, and included as a reference parameter. Since the flight attitude parameters were obtained from the 1553 Bus at 33 Hz, significantly fewer data points went into these averages. Nonetheless, they were averaged on a revolution-by-revolution basis and are suitable for examining relationships between the transmission's vibration output characteristics and the aircraft attitude state.

In order to perform analyses on an experiment-wide basis, the second stage of data reduction involved consolidating selected parameters into a single experiment data matrix (EDM), with groups of rows derived from the different SMs. Each row in the EDM is referred to as a "case." Based on a preliminary analyses, it was decided that data collected from condition G, "Flat Pitch on Ground," would be set aside for other uses, and was therefore eliminated. This reduced the number of SMs involved to 160. Since four hover recordings were made during each Phase, it was further decided to discard the last hover for each pilot, so that each flight condition was uniformly represented by three ordered observations in the analyses. This reduced the number of SMs involved to 156. Finally, so as to obtain information reflecting time-series variability, summary statistics in the EDM were computed separately for each successive group of 28 revolutions, making a total of six ordered "replications" for each of the 156 records.[4] For each of the resulting 936 cases in the EDM, the average number of "runs" above and below the 28 revolution median was also retained for

[4] Extra revolutions were discarded.

testing stationarity of the acceleration and torque data [6].[5]

Data Preparation

Principal Components Analysis

For research purposes tri-axial accelerometers were used to collect vibration data. This provided the flexibility of consolidating the data in any number of arbitrary ways, or rotating the recording axes at will. For the present investigations, the x, y, and z data for each accelerometer were decorrelated using principal components analysis (PCA) techniques. This was done separately for each phase of the experiment, treating the data as a whole, as opposed to each treatment condition. The first principal component may be regarded, therefore, as a single direction vector analogous to an optimally oriented single-axis accelerometer.[6] Normalized PCA scores were retained in the EDM for the three orthogonal components. Based on Scheffé's [7] development of Analysis of Variance procedures for testing the equality of treatment *variances*, rather than treatment means, the natural logarithms of the RMS data were computed prior to applying PCA.[7] All subsequent analyses, therefore, were performed on the three PCA scores, which will be referred to as PC-1, PC-2, and PC-3, respectively in the remainder of the paper.

Stationarity Analyses

A major concern for meaningful analysis of vibration data is the extent to which the recorded time-series are *stationary*—meaning, the extent to which the statistical properties of the series remain invariant over the recording interval. This problem is a particularly relevant issue for HUMS since it is necessary to record over long time periods (e.g., 30 sec.) to obtain sufficient data for several types of planetary signal analysis.

In order to evaluate stationarity on an experiment-wide basis, a standard non-parametric runs test [8] was performed for each of the cases in the EDM.[8] As mentioned above, principal component scores above and below the median were used to determine the number of runs, which is equivalent to evaluating the probability of obtaining the observed runs for 28 observations from a binomial distribution with p = 0.50. Since there were 72 cases for each maneuver, a convenient figure of merit for maneuver stationarity is the percentage of cases that were not found to be significant. It should be kept in mind, therefore, that stationarity represents the "null-hypothesis," which is only inferred based on the *absence* of significant non-stationarity.

Table 5 shows the percentage of stationarity for time-series obtained from the tri-axial accelerometer located at the planetary ring gear during both phases of the experiment, i.e., channels 1-3. The average percentage of cases that were stationarity is 68.58%. Since 72 tests were made in each instance, somewhat less than one significant finding would be expected purely by chance based on $\alpha = 0.01$. It is clear, therefore, that these flight data contain a very high proportion of non-stationary records, a circumstance that would be helpful to mitigate in real-time HUMS because spurious results could be obtained.

Fortunately, it is also apparent that nonstationarity was not the same across maneuvers. Several flight conditions, most notably forward and sideward flight, were severely nonstationary. *Low-and high-power forward climb* conditions, however, were highly stationary—98.48% and 91.67% respectively. We speculate that this was due to a constant rotor load and lifting on the mast during these maneuvers, which induced a relatively constant set of input forces to the transmission. Torque variability was also lowest during these maneuvers, which is consistent with this reasoning.

---

[5] Runs were averaged across the x, y, z axes.

[6] The first principal component is "optimal" in the sense of maximizing the total variance in 3-space. The direction vector calculated for the current analysis, however, does not necessarily correspond with the physical direction of an optimal single-axis accelerometer, although it might have been computed from the raw data.

[7] The authors acknowledge transgressing certain underlying statistical assumptions in the use of this procedure.

[8] Based on inspection of torque prior to this analysis, one observation of Maneuver E, Pilot 2 (6 cases) was eliminated as an obvious outlier. Hence, the total number of cases was 630.

Table 5: Stationarity Based on Runs Tests for Accelerometer A

	MANEUVER	Count	Percent	Cases
A	Forward Flight, Low Speed	45	62.50	72
B	Forward Flight, High Speed	38	52.78	72
C	Sideward Flight Left	30	41.67	72
D	Sideward Flight Right	29	40.28	72
E	Forward Climb, Low Power	65	98.48	66
F	Forward Descent, Low Power	50	69.44	72
H	Hover	64	88.89	72
I	Hover Turn Left	58	80.56	72
J	Hover Turn Right	42	58.33	72
K	Coordinated Turn Left	45	62.50	72
L	Coordinated Turn Right	56	77.78	72
M	Forward Climb, High Power	66	91.67	72
N	Forward Descent, High Power	48	66.67	72
	AVERAGE		68.58	

(α = .01)

Comparisons using Regression and Analysis of Covariance

A fixed-effects ANCOVA was used to determine the relative importance of the various treatment conditions, and the degree to which flight attitude parameters accounted for variability in the vibration scores. A fixed-effects model was used because none of the experimental factors, possibly with the exception of "pilots", was sampled randomly from a larger population for which generalizations would make sense. An attractive feature of the simple fixed-effects model was also that it allows for a partitioning of the total sum-of-squares around the global mean of the experiment on an additive basis.

Total SS = Covariate SS + Main Effects SS + Interaction SS + Error

Thus, it is a particularly useful tool for putting the relative contributions of the various numerical and category factors into global perspective.

Referring to the causal model described in Figure 3, it would have been desirable, to have direct measures of all *essential* inputs {I} to the transmission. Unfortunately, it is still largely a matter of conjecture as to what this basic set might be, and of those suggested in the diagram only engine torque was measured directly. Based on observations made during the stationarity analysis, however, it was postulated that the flight parameters should correlate with transmission input forces, particularly those that might have a direct relationship to mast lifting, e.g., rate-of-climb, or mast bending, e.g., pitch-angle, and airspeed.[9] For this reason, the recorded flight parameters were treated as covariates. Since the three principal component scores are, by definition, orthogonal, and might possibly yield different insights into the nature of transmission vibrations in 3-space, separate analyses were conducted for each of them. Finally, based on an initial exploratory analysis, it was decided to retain only two-way interaction terms and pool the largely non-significant higher-order interactions with residual variance.

In the particular version of ANCOVA that was used here, the linear regressions of the covariates are removed first. This makes the analysis identical to first calculating a multiple-regression using the covariates as predictor variables, and then performing a simple multi-factor analysis-of-variance on the unpredicted portion, i.e., the residual. The three regression analyses for the principal component scores are summarized in Table 6. These will be discussed in conjunction with the main ANCOVA, which also summarizes analyses of each of the three principal component scores (Table 7). In both tables the conventional F-ratio information is omitted because they can be calculated simply by dividing a particular sum-of-squares by the total sum-of-squares. Typical α-probabilities are also suppressed in favor of an asterisk which simply indicates whether the effect was "significant" at the α = 0.01 level.

[9] Mast bending is expected to be minimal with an articulated rotor and more pronounced with a rigid rotor.

Table 6: Multiple Regression and Beta Weights for Aircraft Attitude on Three Principal Component Scores

	PC-1	PC-2	PC-3
R	0.956 *	0.528 *	0.140
R Square	0.914	0.279	0.020
Variable $\{A_j\}$	**Beta**	**Beta**	**Beta**
Airspeed	0.042 *	-0.050	0.053
Altitude	0.013	-0.039	0.047
Bank Angle	-0.016	0.036	-0.034
Heading	-0.036 *	0.103 *	0.019
Pitch Angle	-0.060 *	-0.278 *	0.103
Climb Rate	0.041	-0.570 *	-0.074
Rotor RPM	0.017	0.138 *	-0.078
Torque	0.958 *	0.556 *	-0.032

* significant at the α = 0.01 level

Interpretation of Results

Regression Analyses

The most striking aspect of the combined analyses is the massive amount of experimental variance accounted for by torque—91.4% for PC-1 scores (Table 6). This was not completely unexpected considering many earlier results obtained from test-rigs [4], but it is still rather impressive. In Table 6, the square of the regression coefficient (R Square), is a measure of explained variance. It is exactly the same value as the "Percent Total SS" attributed to covariates seen in Table 7. It is interesting to note that the R Square of torque drops to 27.9% for PC-2, and, has only 2% predictive value for PC-3.

Beta coefficients shown in Table 6 are the weights calculated by least-squares for the three multiple regression equations using standardized values.[10]

$$PC_i = \sum_{j=1}^{k} \beta_{ij} A_{ij} + c_i$$

Symbolically,

where the β-coefficients weight the aircraft attitude parameters $\{A_j\}$ for linear prediction of the i^{th} principal component, with c_i as the intercept.

[10]This transforms the variables into standard deviation units from their respective sample means. It is a helpful procedure for understanding the relative contribution of factors that were not measured in the same units.

With regard to the PC-1 regression equation, therefore, torque has the largest predictive weighting (0.96) and the other flight variables are almost equally represented at very low levels. However, for the PC-2 regression equation torque weighting diminishes (0.56) and rate-of-climb takes on an equally important predictive role (0.57). Pitch angle and rotor RPM also increase in relative importance. Thus, it may be concluded that the first two principal component axes contain somewhat different vibration information. The flight parameters have almost no predictive relationship to PC-3, which has a very small amount of total variance.

Principal Component Comparisons

Before proceeding with a discussion of individual category effects in the analysis-of-covariance (Table 7) it is interesting to note that once covariate regression is removed, PC-1 and PC-2 retain similar amounts of variance to be distributed between the main effects and 2-way interactions. Orthogonalizing the tri-axial data by principal component analysis, in effect, brings about a consolidation of most of the torque-induced vibration energy onto the first component (90.66%). Also, PC-2 primarily accounts for *main effects* variance (63.80%), and PC-3 primarily accounts for *2-way interaction* variance (32.57%). On a general basis, therefore, it would appear that PCA systematically shifts higher-order interactions to the higher principal components. In view of the fact that in PCA each axis accounts successively for the largest amount of remaining variance, this is quite understandable.

In effect, PCA and ANCOVA are simply two different ways of partitioning variance. In this experiment, since greater variance is associated with covariates than with main effects, this shows up on the first axis. Since greater variance is also associated with main effects than with 2-way interactions, this shows up on the second axis, and so forth. Finally, it may be noted that the percentage of residual (unexplained) variance systematically increases from PC-1 (2.59%) to PC-3 (46.82%).

Table 7: Partitioning of Sum of Squares by Principal Component

Source of Variation		PC-1		PC- 2		PC- 3	
	df	Sum of Squares	Percent Total SS	Sum of Squares	Percent Total SS	Sum of Squares	Percent Total SS
Covariates	8	558.778	91.40 *	10.977	27.85 *	0.018	1.97
TORQUE	1	554.282	90.66 *	0.007	0.02	0.003	0.33
RATE OF CLIMB	1	0.552	0.09 *	7.690	19.51 *	0.000	0.00
PITCH ANGLE	1	2.832	0.46 *	2.028	5.15 *	0.003	0.33
AIRSPEED	1	0.165	0.03 *	0.061	0.15 *	0.001	0.11
ALTITUDE	1	0.030	0.00	0.095	0.24 *	0.003	0.33
BANK ANGLE	1	0.125	0.02	0.214	0.54 *	0.002	0.22
HEADING	1	0.643	0.11 *	0.221	0.56 *	0.001	0.11
ROTOR RPM	1	0.148	0.02 *	0.661	1.68 *	0.005	0.55 *
Main Effects	21	27.497	4.50 *	25.143	63.80 *	0.171	18.75 *
MANEUVER	12	26.092	4.27 *	24.938	63.28 *	0.139	15.24 *
ORDER	2	0.504	0.08 *	0.010	0.03	0.017	1.86 *
PILOT	1	0.024	0.00	0.185	0.47 *	0.003	0.33
SET	1	0.818	0.13 *	0.000	0.00	0.004	0.44 *
REPLICATION	5	0.059	0.01	0.010	0.03	0.007	0.77
2-Way Interactions	133	9.239	1.51 *	1.313	3.33 *	0.297	32.57 *
MANEUVER ORDER	24	4.771	0.78 *	0.425	1.08 *	0.047	5.15 *
MANEUVER PILOT	12	1.254	0.21 *	0.134	0.34 *	0.098	10.75 *
MANEUVER SET	12	0.823	0.13 *	0.529	1.34 *	0.071	7.79 *
MANEUVER REP	60	1.014	0.17	0.133	0.34	0.051	5.59 *
ORDER PILOT	2	0.119	0.02	0.012	0.03	0.000	0.00
ORDER SET	2	0.133	0.02	0.007	0.02	0.007	0.77 *
ORDER REP	10	0.126	0.02	0.014	0.04	0.006	0.66
PILOT SET	1	0.204	0.03 *	0.017	0.04	0.005	0.55 *
PILOT REP	5	0.098	0.02	0.012	0.03	0.004	0.44
SET REP	5	0.030	0.00	0.025	0.06	0.006	0.66
Explained	162	595.514	97.41	37.433	94.99	0.485	53.18
Residual	767	15.858	2.59	1.976	5.01	0.427	46.82
Total	929	611.371	100.00	39.409	100.00	0.912	100.00

* significant at the $\alpha = 0.01$ level

Covariance Analysis

With regard to treatment main effects and two-way interactions, there is good reason to be interested in all of them, but for somewhat different reasons. It was expected, of course, that maneuvers would differ in vibration pattern. This is supported by the fact that maneuver is the strongest overall main effect for the three principal components, accounting for 94.9%, 99.2% and 81.3% respectively of their main effects sum-of-squares. It should be emphasized that these and other differences were obtained after the effect of the aircraft attitudes **{A}** was removed.

The order of observation of the maneuvers was found to be significant in PC-1 and PC-3, but accounted for only a small percentage the total variance. This factor is interesting because fuel depletion systematically lowers the gross weight of the vehicle after each observation during the flight. Based on the current findings, it is probably not a highly critical factor within the range of weight changes that occurred. The significant findings on PC-1 and PC-3, however, do suggest that gross-weight should be taken into account in future HUMS computations.

The pilot factor is statistically interesting for several reasons. First, as one would expect, the two well-trained test-pilots performed individual maneuvers somewhat differently, while not differing substantially on an overall basis. Although the pilot main effect is only significant on PC-2, the pilot-maneuver interactions are significant for all three components, indicating that some maneuvers were performed differently than others. Essentially, these differences tended to balance out and do not appear as significant main effects for PC-1 or PC-3. It should be noted, of course, that although a very small amount of total variance is accounted for by these pilot differences, it would have been highly suspect not to find any at all. Maneuvering control was completely in their hands. What is surprising, and rather encouraging for this type of research, is that pilot differences were so *small* relative to the observed differences in maneuver and other treatments.

A small but significant main effect of set—the two phases of the experiment—is found on PC-1 and PC-3. Significant interactions between set and *pilot* on PC-1 and PC-3 also indicate pilot differences between the two phases of the experiment. It is not clear whether these effects were due to time of year, temperature, climactic variations or simply changes in how the pilots went about their flying tasks.

Finally, the replication variable uniformly has no significant main effect on the three PC scores. An interaction effect with maneuver is found on PC-3, however, which possibly suggests some form of trend difference between the time series obtained on different maneuvers. Overall, this is an agreeable result showing that underlying variance associated with the nonstationary properties of the individual time series, at least as we have grossly represented them in the "replication" variable, are quite small relative to other influences.

DISCUSSION AND CONCLUSIONS

Discussion

This paper has summarized the analysis of rotorcraft flight data and identified statistically significant relationships between several important factors typically related to health and usage monitoring. These include, maneuvering states, aircraft attitude variables, pilot differences, and multi-axis vibrations recorded from the helicopter's main transmission. In terms of the overall objectives set out for this flight research, we are gratified that expectations have been largely met. In hindsight, a few improvements in experiment design might have given even more insight into our research. For example, it might have been better to include an intermediate hover to completely balance ordinal gross weight differences on this condition. This will be done in future studies. As a general outcome, however, the value of obtaining controlled, experimental flight data appears to have been amply demonstrated, and we look forward to comparing flight and test-rig data systematically.

Based on lessons learned from the current study, an OH-58c helicopter at Ames is now being instrumented that will inherit the *HealthWatch* system capabilities, as well as the flight test protocols. Specific comparison studies are also currently under way on the OH-58c test-rig at NASA GRC.

Implications for HUMS

From the perspective of refined HUMS development, this study highlights the reality that in-flight vibrations are largely dominated by torque and torque variability. As a consequence, effective HUMS algorithms must meet the challenge of isolating and identifying embedded diagnostic signals, reflecting internal damage states, well before component failures become so serious as to outweigh torque effects in the vibration signal. In order to do this, we believe that means must be found to select quality data for in-flight analysis, and effective tools must be available to decompose the signals in a meaningful way. Although the present findings certainly require further validation, of the 13 steady-state maneuvers investigated here, it would appear that *forward climb* produced the “best” signals. This is born out not only by the stationarity analyses reported above, but also by the fact that the two forward climb conditions also produced the lowest levels of torque variability—a fact which helps to explain their high degree of stationarity. Armed with this insight, parallel research that is being conducted in-house to develop planetary signal decomposition algorithms, and other algorithms to detect internal damage states, will take advantage of these particular flight recordings for development and testing purposes.

Although our use of tri-axial accelerometers was intended to provide maximum research flexibility, e.g., to synthesize single-axis accelerometers in various angular orientations, the present findings suggest other practical uses for them. For example, in a torque-based environment it is probably desirable to partial out torque effects. This could be achieved by measuring torque directly, as we have done, and then applying some form of linear or non-linear regression to produce a residual signal. Curiously, it might also be achieved by recording from tri-axial accelerometers, performing a principal components analysis, and then using PC-2 or PC-3 for signal detection. As will be recalled, the effects of torque were largely consolidated onto PC-1. Whether this conjecture is valid or valuable is being explored in the laboratory.

Finally, it should be mentioned that during the course of this study we have become even more mindful that internal transmission component failures can only be observed systematically in ground-test facilities. For this reason, signal detection algorithms must necessarily be developed, and evaluated in those environments, particularly to establish their potential “hit-rate” ability. Permanently instrumented research aircraft, such as NASA’s Cobra, OH-58, and UH-60 helicopters, however, will be also needed to evaluate equally important “false-alarm” rates under the full range of normal operating conditions.

Acknowledgments

The authors would like to express their gratitude to Mr. Larry Cochrane, California Signal Processing Associates, Inc. for aircraft instrumentation and raw data reduction. We would also like to thank Ms. Alissa Fitzgerald, of the same organization, for her engineering design and analysis of the accelerometer mounting brackets used in this study.

REFERENCES

1. Hollins, M.L., *The Effects of Vibration Sensor Location in Detecting Gear and Bearing Defects*, 1986, Naval Air Test Center: Patuxent River, MD.
2. Chin, H., K. Danai, and D.G. Lewicki. *Fault Detection of Helicopter Gearboxes Using the Multi-Valued Influence Matrix Method*, in *ASME Winter Annual Meeting*. 1993. New Orleans: American Society of Mechanical Engineers.
3. Hollins, M.L., *Test Bed Defective Component Data*, 1991, Naval Air Test Center: Patuxent River, MD.
4. Zakrajsek, J.J., *A Review of Transmission Diagnostics Research at NASA Lewis Research Center*, 1994, NASA Lewis Research Center: Cleveland.
5. Hess, A., B. Hardman, and C. Neubert. *SH-60 Helicopter Integrated Diagnostic System (HIDS) Program Experience and Results of Seeded Fault Testing*. in *American Helicopter Society 54th Annual Forum*. 1998. Washington: AHS.
6. Bendat, J.S. and A.G. Piersol, *Random Data Analysis and Measurement Procedures*. 1986, New York: Wiley.
7. Scheffé, H., *The Analysis of Variance*. First ed. 1959, New York: Wiley.
8. Siegel, S., *Nonparametric Statistics for the Behavioral Sciences*. 1956, New York: McGraw-Hill.